Journal of Biomaterials Applications
http://jba.sagepub.com/

Biodistribution of ultra small gadolinium-based nanoparticles as theranostic agent: Application to brain tumors

Imen Miladi, Géraldine Le Duc, David Kryza, Aurélie Berniard, Pierre Mowat, Stéphane Roux, Jacqueline Taleb, Pauline Bonazza, Pascal Perriat, François Lux, Olivier Tillement, Claire Billotey and Marc Janier

J Biomater Appl 2013 28: 385 originally published online 24 July 2012
DOI: 10.1177/0885328212454315

The online version of this article can be found at:
http://jba.sagepub.com/content/28/3/385

Published by:
SAGE
http://www.sagepublications.com

Article

JOURNAL OF
biomaterials
applications

Journal of Biomaterials Applications
28(3) 385–394

DOI: 10.1177/0885328212454315
jba.sagepub.com
SAGE

Biodistribution of ultra small gadolinium-based nanoparticles as theranostic agent: Application to brain tumors

Imen Miladi[1], Géraldine Le Duc[2], David Kryza[1,3], Aurélie Berniard[1], Pierre Mowat[1], Stéphane Roux[1,4], Jacqueline Taleb[1], Pauline Bonazza[1], Pascal Perriat[5], François Lux[1], Olivier Tillement[1], Claire Billotey[1,3,*] and Marc Janier[1,3,*]

Abstract

Gadolinium-based nanoparticles are novel objects with interesting physical properties, allowing their use for diagnostic and therapeutic applications. Gadolinium-based nanoparticles were imaged following intravenous injection in healthy rats and rats grafted with 9L gliosarcoma tumors using magnetic resonance imaging and scintigraphic imaging. Quantitative biodistribution using gamma-counting of each sampled organ confirmed that these nanoparticles were rapidly cleared essentially by renal excretion. Accumulation of these nanoparticles in 9L gliosarcoma tumors implanted in the rat brain was quantitated. This passive and long-duration accumulation of gadolinium-based nanoparticles in tumor, which is related to disruption of the blood–brain barrier, is in good agreement with the use of these nanoparticles as radiosensitizers for brain tumors.

Keywords

Gadolinium-based nanoparticles, brain tumour, biodistribution

Introduction

Nanotechnology is considered an emerging technology with significant impact on applications for cancer therapy. There has been a tremendous investment and research effort in recent years, particularly in the field of anticancer drug delivery and medical imaging contrast agents.[1,2]

The current approaches for cancer therapy are numerous, including surgical resection, radiation, and chemotherapy, but results are not satisfactory for all tumors. As an illustration, treatment of glioblastoma, a primary malignant tumor of the brain, remains one of the most challenging cancer issue, as no curative treatment has yet been found.[3] The promises of nanotechnology in cancer research lie in the technique potential of overcoming these limitations for such tumors. Indeed, some nanoparticles are developed for therapeutic purposes[4,5] or for theranostic use.[6]

Our group has developed gadolinium-based nanoparticles (GBNs), which can be detected by imaging modalities used in routine clinical practice, and thus be used as radiosensitizing agents in cancer therapy. GBNs are composed of a core of rare-earth atoms (gadolinium), surrounded by a polysiloxane shell (four silicon atoms/one gadolinium (Gd) atom in this study) that can be used to label specific targeting molecules.

Previous in vitro and in vivo studies demonstrated that the effects of γ and X-rays were enhanced by the

[1]Laboratoire de Physico-Chimie des Matériaux Luminescents, UMR 5620 CNRS, Université Claude Bernard Lyon 1, Villeurbanne Cedex, France
[2]European Synchrotron Radiation Facility, ID 17 Biomedical Beamline, Polygone Scientifique Louis Néel, Grenoble, France
[3]Hospices Civils de Lyon, Service de Médecine Nucléaire, Hôpital Edouard Herriot, Lyon, France
[4]Institut UTINAM, UMR 6213 CNRS, Université de Franche-Comté, Besançon Cedex, France
[5]Matériaux Ingénierie et Science, UMR 5510 CNRS, Villeurbanne Cedex, France

*The authors have contributed equally to the article.

Corresponding author:
Imen Miladi, Laboratoire de Physico-Chimie des Matériaux Luminescents, UMR 5620 CNRS, Université Claude Bernard Lyon 1, Villeurbanne Cedex, France.
Email: melle_miladi@yahoo.fr

presence in the tissue of interest of these GBN since Gd element exhibits a high propensity to absorb these radiations owing to its relatively high atomic number Z.[7,8] DNA strands of cells irradiated after incubation with GBN were obviously more altered than the DNA of cells irradiated incubated without GBN.[9] Moreover, in vivo radiotherapy experiments showed that 9L gliosarcoma bearing rats revealed a longer increase of lifespan (ILS) when they were treated after GBN injection. This in vivo study emphasizes on the importance of the Gd content ratio in tumor and in surrounding healthy tissue which increases with time. The ILS of animals irradiated 20 min after the intravenous injection of GBN is largely greater than the ILS of animals irradiated 5 min after the injection. The temporal evolution of the biodistribution of GBN after intravenous injection is therefore needed for optimizing the effects of GBN applied for radiotherapy.

The present work was designed to evaluate the biodistribution of GBN (4Si/Gd) 20 min and 24 h after the intravenous injection of GBN radiolabeled with Indium111 to healthy rats (control) and 9L gliosarcoma bearing rats. The biodistribution was monitored by SPECT, ex vivo γ counting of the organs, magnetic resonance imaging (MRI) and post-mortem elemental analysis using inductively coupled plasma-mass spectrometry (ICP-MS).

Material and methods

Chemicals

Gadolinium chloride hexahydrate ($GdCl_3$ $6H_2O$, 99.99%), sodium hydroxide (NaOH, 99.99%), tetraethyl orthosilicate ($Si(OC_2H_5)_4$, TEOS (98%), (3-aminopropyl)triethoxysilane ($H_2N(CH_2)_3$-$Si(OC_2H_5)_3$, APTES (99%), sodium chloride (NaCl), triethylamine (TEA, 99.5%), nitric acid (HNO_3, 65%), dimethyl sulfoxide anhydrous ($(CH_3)_2SO$, DMSO, >99.9%) and diethyl ether ($(CH_3CH_2)_2O$, >99%) were purchased from Aldrich Chemical (France). Diethylene triamine pentaacetic dianhydride ($C_{14}H_{19}N_3O_8$, DTPA-ba, >98.0%) was purchased from TCI Europe. Ethanol, diethylene glycol (DEG, 99%), and other organic solvents (reagent grade) were purchased from SDS (France) and used as received. For the preparation of an aqueous solution of NPs, milli-Q water ($\rho > 18\,M\Omega$) was employed. The ultrafiltration was performed using Vivaspin 5000 Da purchased from GE Healthcare.

Synthesis of GBN

The synthesis of GBNs which rests on the encapsulation of Gd oxide core in a thin polysiloxane shell functrionalized by DTPA moieties was described elsewhere.[7] The synthesis is composed of three main steps. First, Gd oxide particles were obtained by precipitation at temperature below 200°C, by applying a modified 'polyol' synthesis.[10] In the second step, a controlled polysiloxane shell growth was induced on the Gd oxide cores (Si to Gd molar ratio: 4) by hydrolysis/condensation of a mixture of TEOS and APTES.[7,8,11] Finally, a post-functionalization was done using DTPA-ba.[7] Typically, a colloidal solution of hybrid nanoparticles in DEG (50 mL, [Gd] = 37 mM) was added into a suspension of DTPA-ba (1.2 eq/Gd) in anhydrous DMSO (60 mL).

The reaction mixture was stirred overnight at room temperature. Then, a mixture of acetone and diethyl ether (1:1, v:v) was poured into the reaction. A precipitate was formed, and a purification step was carried out by an initial centrifugation at 6000 r/min for 5 min and redispersion in ethanol, with subsequent centrifugation (3-fold, 6000 rpm for 10 min). The NPs were then redispersed in Milli-Q water at high concentration. The colloidal solution was transferred into a Vivaspin 5000 Da, and an ultrafiltration was performed. Finally, a lyophilization procedure of GBN was carried out.

GBN characterization

Direct measurement of the size distribution of GBN was performed using the ZETASIZER Nano S (Malvern Instruments, Malvern, UK). The hydrodynamic diameter of the nanoparticles was evaluated by photon correlation spectroscopy (PCS).

Detailed structural and morphological information about GBN were obtained by high-resolution transmission electron microscopy (HRTEM) carried out using a JEOL 2010 microscope.

Determination of the Gd content in a sample was performed by ICP-MS analysis (Varian 710-ES). Before measuring Gd concentration, lyophilized samples of GBN were redispersed in Milli-Q water and dissolved in concentrated nitric acid (1:2500, v/v). The samples were then diluted in HNO_3 (2%; 1:50, v/v).

Radiolabeling of GBN with ^{111}In

For the quantitative study during 14 days, GBN were labeled using Indium-111 (^{111}In) radionuclide. Briefly, 370 MBq of high purity ^{111}In-chloride in diluted hydrochloric acid (Covidien, Petten, Netherland) was added to 1 mL of an aqueous solution of GBN ([Gd] = 100 mM]); ^{111}In links to the DTPA hydrophilic layer of the NPs via coordination bonds.

The mixture was incubated for 30 min at room temperature. GBN-^{111}In was separated from ^{111}In-chloride by PD-10 column (GE Healthcare Bio-Sciences AB,

Uppsala, Sweden), as described in the following steps: The PD-10 column was first washed with 15 mL of 50 mM citrate buffer (pH = 5). The radiolabeling solution was then loaded on the PD-10 column, and fractions of 0.5 mL were eluted with 50 mM citrate buffer (pH = 5). GBN-^{111}In was first eluted. The radioactivity of each fraction was counted using an ionization chamber (Capintec Radioisotope Calibrator CRC-15, Capintec Inc.). Finally, the four fractions with the highest radioactivity were pooled. The solution was then challenged with 200 µL of the complexing chelating agent diethylene triamine pentaacetic acid (DTPA; 20 µmol) for 5 min in order to scavenge potential unbound ^{111}In. Another elution was performed on a PD-10 column using 50 mM citrate buffer (pH = 5) as eluent. The DTPA complex was eluted after GBN-^{111}In. Radiochemical purity was determined using instant thin layer chromatography (ITLC). ITLC of the purified GBN-^{111}In was performed using silica gel plates (Gelman Science Inc., Ann Arbor, MI, USA) in 50 mM citrate buffer (pH = 5) as the solvent and a TLC scanner (MiniGita, Raytest, Isotopenmessgeräte, GmbH, Straubenhardt, Germany) in order to determine the percentage of free ^{111}In-chloride. GBN-^{111}In remained at the origin, whereas the residual ^{111}In-chloride migrated with an Rf of 0.8.

Stability of radiolabeled GBN-^{111}In was evaluated for 4 h, 24 h, 7 days and 14 days.

Animals

All operative procedures related to animal care were strictly in line with the Guidelines of the French Government with licenses 693881416/380825, and the protocol had been approved by the "*Comité d'Ethique de l'Université Claude Bernard*", Lyon, France.

Adult male Fisher 344 rats (180–280 g) were obtained from Charles River Laboratory (L'Arbresle, France). All animals were housed under standard environmental conditions (free access to food and water and a 12/12 h light/dark cycle) and acclimated for at least 48 h before experimentation.

Orthotopic gliosarcoma rat model

The 9L gliosarcoma cell line[12] was established according to Benda et al.[13] Cells were grown with complete medium at 37°C. Rats were anesthetized with 4% isoflurane inhalation followed by an intraperitoneal injection of a mixture of ketamine (64.5 mg/kg) and xylazine (5.4 mg/kg), and then placed on a stereotactic head holder (model 900, David Kopf Instruments, Tujunga, USA). At Day 0, 10^4 cells were suspended into 1 µL DMEM with antibiotics (1%), then injected using a 1-µL Hamilton syringe through a burr hole in the right caudate nucleus (9 mm anterior to the ear-bars, i.e., at bregma site, 3.5 mm lateral to the midline and 5.5 mm depth from the skull).[14]

Biodistribution study

Blood circulation half-life of radiolabeled GBN. Blood circulation half-life was evaluated in healthy rats (n = 3). After IV injection of 5 MBq GBN-^{111}In in rats, blood samples were removed from caudal vein at different time intervals (5 min, 10 min, 20 min, 30 min, 60 min, 120 min and 240 min). Samples were weighed and counted for 5 min in gamma scintillation counter. Data points were fit to an exponential decay function.

Imaging study

SPECT/CT imaging. Acquisitions were obtained using a small animal Nano-SPECT/CT system (Bioscan, Washington, DC, USA). First, static SPECT acquisitions were performed for 5 min after IV injection of GBN-^{111}In [2 to 10 MBq] in 25 healthy rats and 12 rats bearing 9L gliosarcoma tumors. Rats were in supine position placed directly on planar collimator set in order to verify the quality of the injection and analyze organ nanoparticle uptake.

Then, X-ray CT (tube voltage of 55 kVp, exposure time of 1000 ms and 180 projections) and SPECT acquisitions (15 000 cps per projection/20 projections) were performed before sacrifice using a rat whole-body high-resolution aperture. All image data was reconstructed and analyzed using In Vivo-Scope (Bioscan, Washington, DC, USA). Rats were sacrificed and sampled at the end of the experiment.

Magnetic resonance imaging. Rats bearing 9L gliosarcoma tumors (n = 4) underwent MRI examination at Day 14 following 9L gliosarcoma grafting. Images were acquired via a 7-Tesla imaging system (Biospec; Bruker, Ettlingen, Germany) equipped with 400 mT/m gradient. Anesthesia was induced with 3–4% isoflurane inhalation and maintained with 1.5–2% isoflurane inhalation in a mixture of O_2/N_2 (25%/75%).

In a first step, T_2-weighted images were acquired with a Turbo RARE Spin Echo sequence (TE = 36 ms, TR = 4200 ms, field of view = 2.56 cm, matrix = 256 × 256, and slice thickness = 0.65 mm) prior to injection in order to confirm proper growth of the 9L gliosarcoma grafting.

Second, T_1-weighted FLASH images (TE = 3.6 ms, TR = 86.07 ms, field of view = 2.56 cm, matrix = 256 × 256 and slice thickness = 0.65 mm) were acquired as a baseline before GBN injection. Then, dynamic series of transverse slices centered on

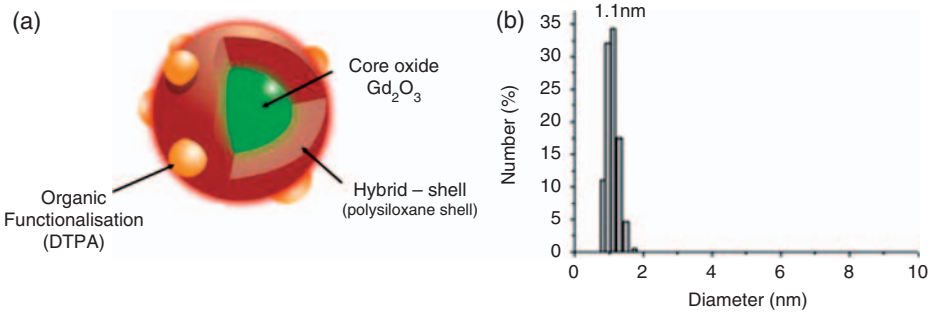

Figure 1. Structural depiction of gadolinium-based nanoparticles (GBN) (a) and core size distribution (b) obtained by high-resolution transmission electron microscopy (HRTEM).

the rat brain, obtained using a T_1-weighted multi-slice-multi-echo (MSME) sequence (TR/TE = 113.4/10.6 ms, slice thickness = 1.5 mm, field of view = 5 cm and matrix = 256 × 256) were acquired. During the fourth repetition of dynamic acquisition imaging, rats were injected with 1.4 mL of GBN suspension with a Gd equivalent concentration of 40 mM (dose used in gliosarcoma radiosensitizing study[7]).

A region of interest (ROI) was drawn in order to delineate the whole tumor area, and the signal in this area was measured on each image. Positive enhancement of the signal (EHC) in tumor area was calculated as $(St–S_0)/S_0$, where St is the signal intensity value measured for each image following injection, and S_0 the signal value prior to injection. EHC curves in relation to time were generated.

Ex vivo biodistribution studies

Ex vivo gamma counting. Radiolabeled nanoparticles in HEPES buffer containing 150 mM NaCl were injected intravenously through the saphenous vein in rats after anesthesia (intraperitoneal injection of xylazine/ketamine (64.5/5.4 mg kg^{-1})) had been administered.

Twelve rats grafted with 9L gliosarcoma cells were injected with radiolabeled GBN 10 days after tumor grafting. Quantitative tissue distribution of radiolabeled GBN in rats was evaluated 20 min (n = 8) and 24 h (n = 4) after injection and organs of interest were collected (heart, lungs, spleen, liver, brain, kidneys, bones, muscles, skin and cadaver). Tumor and healthy brain (controlateral hemisphere and brain tissue surrounding tumor) were separated prior to be counted for 5 min in gamma scintillation counter (Wizard gamma counter, Perkin-Elmer, USA) in order to evaluate the percentage of GBN accumulation in 9L gliosarcoma tumors.

Healthy rats were sacrificed at 20 min (n = 4), 1 h (n = 5), 2 h (n = 3), 4 h (n = 3), 24 h (n = 5) and 14 days (n = 5) after injection and organs of interest such as the heart, lungs, spleen, liver, brain, kidneys, bones, muscles, skin and cadaver were collected. Urine and feces were also collected each day and weighed and counted for 5 min in automatic gamma counter. Tissue distribution was expressed as a percent injected dose per gram of organ (%ID/g). The injected dose was calculated by adding activity of all organs, cadaver, and excretions (feces and urine). Renal and hepatobiliary eliminations were evaluated by measuring respectively urine and feces activities.

Ex-vivo ICP-MS. To determine the particle distribution in the brain at 20 min after GBN injection, ex vivo elemental analyses by ICP-MS were performed separately on the right and left hemispheres collected from rats bearing 9L gliosarcoma tumors (n = 5). Samples were digested for 72 h at 90°C in teflon beakers with Suprapur® 69% nitric acid on ceramic hot plates. When complete dissolution was achieved, samples were diluted with 18 MOhms resistivity water. Aqueous In and Re solutions were added to each sample as internal standards in order to correct possible sensitivity drift of ICP-MS. ICP-MS measurements were conducted on Thermo Electron serie X2. Reported Gd ICP-MS signals represent the average of five replicates. Typical relative standard deviation was approximately 3% or less per sample. Gd concentrations were back-calculated taking into account dilution factor and sensitivity drift correction.

Results

GBN characterization

Elemental analysis performed by ICP-MS revealed that Si to Gd and DTPA to Gd ratios were of 3.5 and 0.87, respectively. The hydrodynamic diameter of Gd oxide nanoparticles embedded in the polysiloxane shell measured by PCS does not exceed 2 nm. According to HRTEM and PCS, cores have a size of 1.1 ± 0.6 nm (Figure 1) so that the surrounding polysiloxane shell thickness was of 0.5 nm. Zeta potential of GBN at

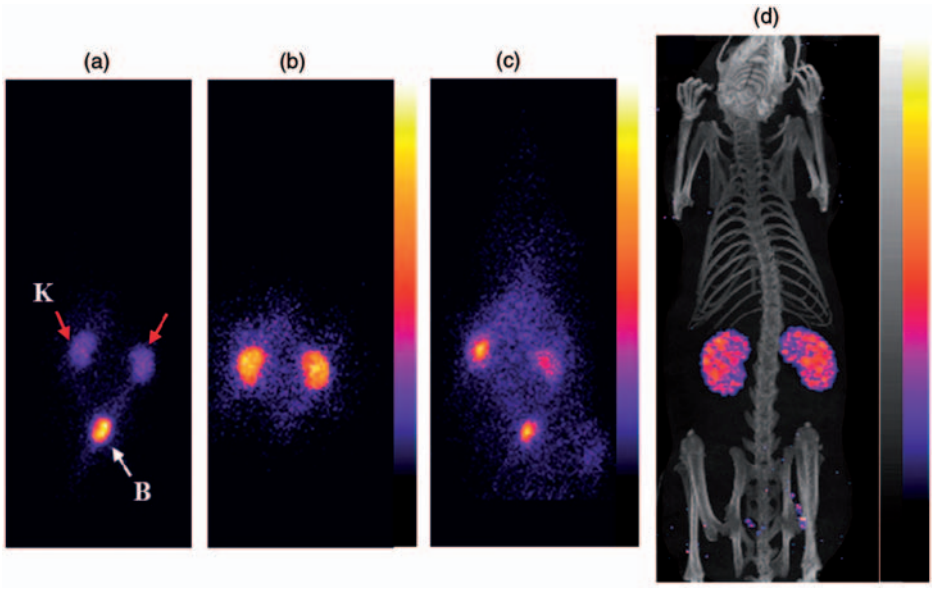

Figure 2. SPECT/CT in vivo imaging in rats: (a) Planar scintigraphic images of a healthy rat acquired 5 min and (b) 24 h after IV injection of gadolinium-based nanoparticles (GBN)–^{111}In. (c) Planar scintigraphic image of a gliosarcoma bearing rat acquired 5 min after IV injection of GBN-^{111}In. (d) Coronal slice of tomographic scintigraphy and X-ray CT of the whole body of gliosarcoma bearing rat acquired 24 h after GBN injection. Red arrows indicate the kidneys (K) and white arrow indicates the bladder (B).

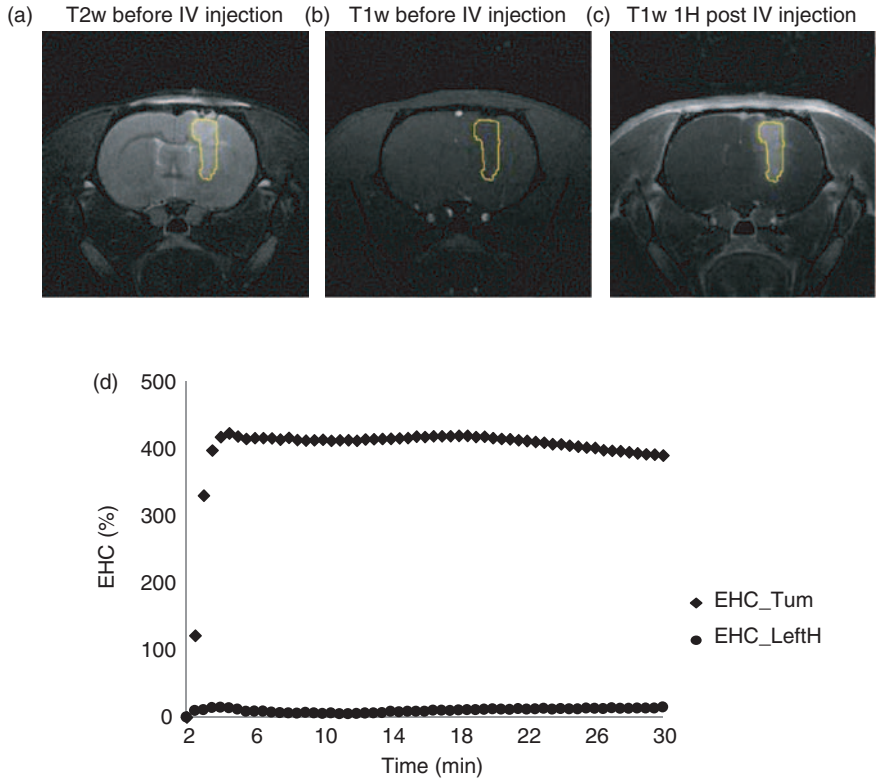

Figure 3. T2- and T1-weighted axial images of 9L gliosarcoma tumor before (a and b) and after (c) injection of gadolinium-based nanoparticles (GBN). (a) Tumor is detectable in the T2-weighted axial slices (yellow region of interest [ROI] delineates the tumor). (c) Tumor is clearly visible up to 1 h after injection of GBN due to the homogeneous dispersion of GBN. (d) Time enhancement of the signal (EHC) curve generated from tumor (diamonds) and healthy brain tissue in the left hemisphere (circles).

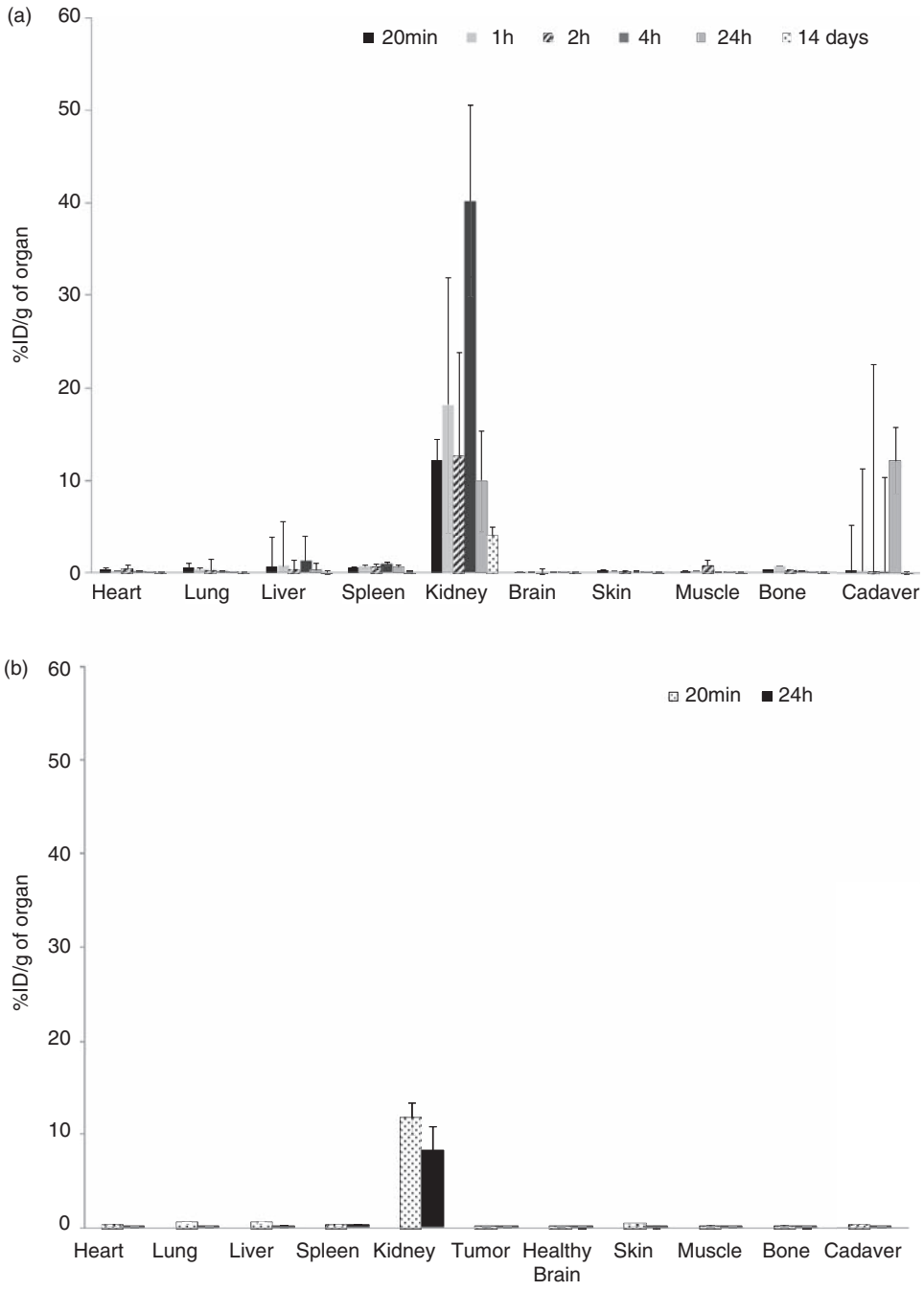

Figure 4. Radioactivity in collected organs at different intervals of time in healthy rats (a) and 9L grafted rats (b) obtained by ex vivo gamma counting following intravenous administration of radiolabeled gadolinium-based nanoparticles (GBN). Data is expressed as percent injected dose per gram of tissue (%ID/g).

pH 7.4 was close to 0 mV. The ability of GBN to enhance MRI T_1 contrast was evidenced thanks to their high longitudinal relaxivity r_1 ($r_1 = 9.4\,s^{-1}.mM^{-1}$ at 60 MHz) and transverse to longitudinal ratio r2/r1 of 1.13 measured by nuclear magnetic relaxation spectroscopy.[7]

Radiolabeling stability

Following purification, radiochemical purity exceeded 99%. After 4 h, 24 h, 7 days and 14 days incubation, radiochemical purity was greater than 99%, 98%, 93%

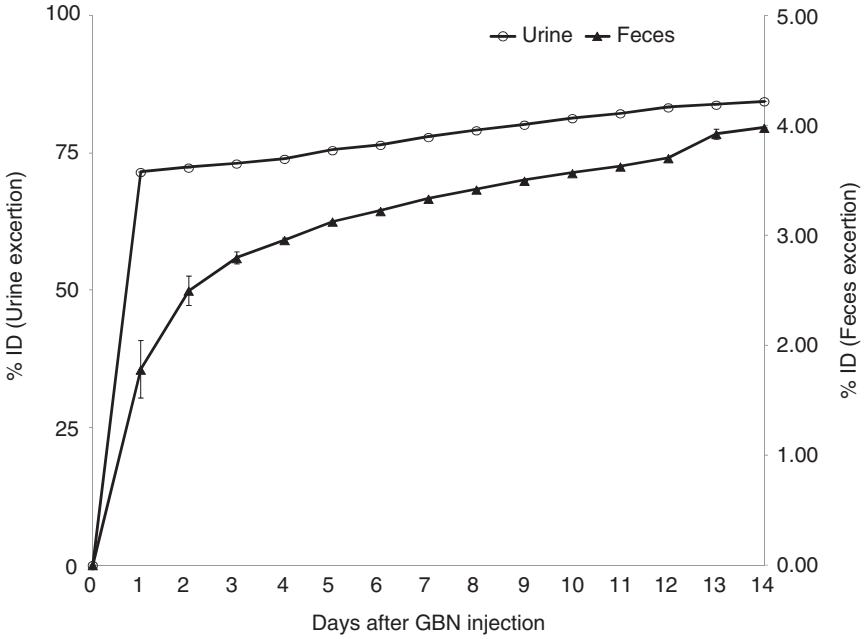

Figure 5. Elimination of radiolabeled gadolinium-based nanoparticles (GBN) after IV injection in healthy rats. Values are expressed as percentage of cumulative activity measured in urine (circle) and feces (triangle) per injected dose (%ID). Data is expressed as mean ± SD.

and 91%, respectively. This indicated that GBN-^{111}In remained stable at least for 14 days.

Imaging study

SPECT/CT imaging. Figure 2 shows in vivo images of organs following intravenous administration of radiolabeled GBN to healthy rats and gliosarcoma bearing rats. High levels of radioactivity were observed rapidly in kidneys and bladder with the absence of significant uptake in other tissues.

Magnetic resonance imaging. Following intravenous injection of GBN, T_1-weighted images as well as the signal enhancement curve showed a continuous signal increase in tumor ROI during the first 3 min post-injection followed by a stable plateau (EHC = 300% to 400%) observed for 30 min at least, as shown in Figure 3. A mean MRI EHC ratio between control hemisphere (LH) and hemisphere bearing the tumor (right hemisphere; RH) was of 13.3 ± 1.6 with an EHC in LH and RH of 9.2 ± 0.9 and 123.6 ± 27.5, respectively.

Ex-vivo biodistribution study

Ex-vivo gamma counting. Twenty minutes after GBN injection, tumor uptake was higher than the one of healthy brain (HB). In each gliosarcoma bearing rat (n = 8), an increase of radiolabeled GBN accumulation in the tumor was observed. A ratio of 1.16 ± 0.10 was found in percentage injected dose per gram of tissue between tumor and healthy brain.

Moreover, GBN biodistribution was very similar between healthy and diseased rats 20 min and 24 h after injection in the other organs as shown in Figure 4.

The blood circulation half-life of radiolabeled GBN was evaluated at 32 ± 4 min. Renal and liver excretions of GBN were evaluated by measuring urine and feces activity as shown in Figure 5. GBN were rapidly eliminated through renal excretion with 71.5 ± 0.1% ID, compared to feces excretion with 1.8 ± 0.3% ID 24 h after IV injection.

High levels of radioactivity were observed in the kidneys after GBN IV administration (12.15% ID/g of organ at 20 min) and were reduced from 9.88% at 24 h to 4.07% at 14 days (Figure 4(a)). No significant uptake of GBN was observed in liver, as well as in spleen, lungs and bones.

ICP-MS analysis. The Gd content within the RH bearing the tumor compared to the Gd content in the contralateral hemispheres (LH) exhibited a ratio of 1.25 ± 0.19 with a mean Gd content in RH and LH of 2.9 ± 0.7 and 2.3 ± 0.6 µg of Gd per gram of tissue, respectively. These results showed that the ICP-MS measurements were in good agreement, thereby validating gamma counting results.

Discussion

The development of in vivo imaging methods allows for a better understanding of the anatomy, physiology and function of the brain but also for a better visualization of the biodistribution of drugs. This provides an opportunity to localize specific pathologic targets, but also to assess whether a specific therapeutic agent is distributed efficiently within the target volume. In this context, we have developed a new class of therapeutic GBNs that can be detected using several modalities, allowing us to analyze their distribution within the brain and their bioelimination.

This study demonstrated that GBN can efficiently accumulate in 9L gliosarcoma tumors grafted in rat brains after IV injection. This accumulation can be accounted by the ability of GBN to cross the blood–brain barrier (BBB) of rats bearing 9L gliosarcoma tumors.

The BBB prevents larger (>400 Da) molecules from entering the brain parenchyma, thereby protecting it from toxic foreign substances.[15] Owing to the presence of the BBB, drug delivery to the brain by systemic routes remains challenging to achieve an effective diagnosis and treatment.[16,17] But in the case of brain tumors, the BBB or blood tumor barrier becomes abnormal because of defects in inter-endothelial tight junctions that correlate with increasing malignancy in human gliomas.[18,19] Therefore, the systemic delivery of drugs for treatment of brain cancer may become possible. Brigger et al. have shown that following an IV injection of (PEG)-coated hexadecylcyanoacrylate (PHDCA) NPs or PHDCA NPs into intracranial 9L gliosarcoma-bearing rats, both types of nanospheres were accumulated in the 9L gliosarcoma tumors in rats, whereas no accumulation of these nanospheres was observed for healthy animals.[20]

Our gamma counting data demonstrated that GBN can reach tumor tissue since the difference in the uptake of radiolabeled GBN between the tumor and healthy brain is by a factor of 1.16 after 20 min of IV injection.

This accumulation in tumor confirms the GBN ability to cross altered and leaky BBB in 9L gliosarcoma rats. Gamma counting results correlated well with ICP-MS results.

Even though this moderate GBN accumulation was sufficient to provide an optimized concentration of GBN so as to obtain a radiosensitizing effect as previously reported,[7] these GBN can be specifically targeted allowing for an increased uptake by cancer cells and thus an increased accumulation in the tumor region.

Moreover, ex vivo gamma counting performed 24 h after injection evidenced an interesting ratio between tumor and healthy brain, but with a decrease in % ID/g of tissue in tumor as well as in healthy brain. This accumulation suggests that a fractionated therapy can be envisaged to improve therapy effectiveness in presence of GBN, since multifraction radiation treatment is considered to be advantageous for tumor control because greater nonrepairable damage is induced per unit dose in tumor cells and increased tolerance of the surrounding healthy tissues to fractionated doses.[21,22]

Although the BBB was disrupted by the presence of a brain tumor, the efficacy of drugs administered by a systemic injection was still limited by poor penetration through this barrier.[23] Moreover, many solid tumors exhibit a high interstitial fluid pressure, which represents also a barrier to transcapillary transport and inhibits the homogeneity of therapeutic agent distribution in tumor tissues.[24] All these restrictions can be avoided by targeting which can actively enhance nanoparticles accumulation.[25,26] Liu et al. have evidenced that Magnetic Targeting increased magnetic nanoparticles (MNPs) accumulation by a factor of 11 in brain tumor site, thereby increasing the therapeutic dose delivered beyond that obtainable by passive diffusion.[25]

Our study reveals excellent GBN contrast enhancing properties observed in the tumor area until 1 h following the injection (Figure 3), with a mean MRI signal ratio between control hemisphere and hemisphere bearing the tumor of 13.3. This confirms that GBNs are able to reach the tumor due to BBB disruption. The presence of Gd inside the tumor provides a strong positive contrast and allows for high-resolution in vivo images.[7,8] However, MRI provides an increase of signal due to the positive contrast allowed by the presence of GBN but do not allow quantifying the real concentration of GBN in tumor. The GBN concentration is quantified, thanks to gamma counting and ICP-MS analysis.

The contrast difference between tumor and surrounding healthy tissues (Figure 3(c)) can be accounted for by a denser vascularization of the tumor, as its rapid growth requires the recruitment of additional blood vessels for delivering a large amount of nutriments and oxygen to the tumor.[15]

In this study, no adverse effects were evidenced on the large number of injected rats. No death was attributed to nanoparticles injection.

The presence of GBN in kidneys and bladder attested that GBN clearance following IV injection was performed via renal excretion as major route. In fact, our gamma counting data evidenced a high rate of renal elimination of GBN with more than 90% and 95% of GBN eliminated, respectively, 24 h and 14 days after IV injection (Figure 4). The renal clearance of GBN is favored by their small hydrodynamic

diameter, which is consistent with similar nanosized particles,[27] and should avoid any long-term toxicity.[28,29]

Conclusion

Our biodistribution study demonstrated that a novel agent (GBN-4Si/Gd) was able to accumulate in orthotopic 9L tumors until 24 h after intravenous injection, and demonstrated favorable in-vivo kinetics. This passive accumulation in tumor in relation to BBB disruption is in good agreement with the use of these nanoparticles for the treatment of malignant brain tumors.

In conclusion, these GBN are novel objects with very promising imaging properties and with favorable biodistribution which enable their use simultaneously as diagnostic and therapeutic agents.

Funding

This research was funded by the Agence Nationale de la Recherche (ANR-PNANO-05), Nano-H SAS and Clara-Lantharad.

Acknowledgements

We thank Mr. Benoit DENIZOT for assistance in preparation of this manuscript and CLYM for access to microscope JEOL 2010.

References

1. Kim KY. Nanotechnology platforms and physiological challenges for cancer therapeutics. *Nanomedicine* 2007; 3(2): 103–110.
2. Ferrari M. Cancer nanotechnology: opportunities and challenges. *Nat Rev Cancer* 2005; 5(3): 161–171.
3. Mannino M and Chalmers AJ. Radioresistance of glioma stem cells: intrinsic characteristic or property of the microenvironment-stem cell unit? *Mol Oncol* 2011; 5(4): 374–386.
4. Steiniger SCJ, Kreuter J, Khalansky AS, et al. Chemotherapy of glioblastoma in rats using doxorubicin-loaded nanoparticles. *Int J Cancer* 2004; 109(5): 759–767.
5. Acharya S and Sahoo SK. PLGA nanoparticles containing various anticancer agents and tumour delivery by EPR effect. *Adv Drug Deliv Rev* 2011; 63(3): 170–183.
6. Sumer B and Gao J. Theranostic nanomedicine for cancer. *Nanomedicine (Lond)* 2008; 3(2): 137–140.
7. Le Duc G, Miladi I, Alric C, et al. Toward an image-guided microbeam radiation therapy using gadolinium-based nanoparticles. *ACS Nano* 2011; 5(12): 9566–9574.
8. Fizet J, Rivière C, Bridot JL, et al. Multi-luminescent hybrid gadolinium oxide nanoparticles as potential cell labeling. *J Nanosci Nanotechnol* 2009; 9(10): 5717–5725.
9. Mowat P, Mignot A, Rima W, et al. In vitro radiosensitizing effects of ultrasmall gadolinium based particles on tumour cells. *J Nanosci Nanotechnol* 2011; 11(9): 7833–7839.
10. Bazzi R, Flores MA, Louis C, et al. Synthesis and properties of europium-based phosphors on the nanometer scale: Eu2O3, Gd2O3:Eu, and Y2O3:Eu. *J Coll Interface Sci* 2004; 273(1): 191–197.
11. Bridot J-L, Faure A-C, Laurent S, et al. Hybrid gadolinium oxide nanoparticles: multimodal contrast agents for in vivo imaging. *J Am Chem Soc* 2007; 129(16): 5076–5084.
12. Coderre J, Rubin P, Freedman A, et al. Selective ablation of rat brain tumors by boron neutron capture therapy. *Int. J. Radiat. Oncol. Biol. Phys* 1994; 28(5): 1067–1077.
13. Benda P, Someda K, Messer J, et al. Morphological and immunochemical studies of rat glial tumors and clonal strains propagated in culture. *J Neurosurg* 1971; 34(3): 310–323.
14. Kobayashi N, Allen N, Clendenon NR, et al. An improved rat brain-tumor model. *J Neurosurg* 1980; 53(6): 808–815.
15. Pardridge WM. Drug and gene delivery to the brain: the vascular route. *Neuron* 2002; 36(4): 555–558.
16. De Jong WH and Borm PJA. Drug delivery and nanoparticles: applications and hazards. *Int J Nanomedicine* 2008; 3(2): 133–149.
17. Pardridge WM. The blood-brain barrier: bottleneck in brain drug development. *NeuroRx* 2005; 2(1): 3–14.
18. Segal MB. The choroid plexuses and the barriers between the blood and the cerebrospinal fluid. *Cell Mol Neurobiol* 2000; 20(2): 183–196.
19. Papadopoulos MC, Saadoun S, Binder DK, et al. Molecular mechanisms of brain tumor edema. *Neuroscience* 2004; 129(4): 1011–1020.
20. Brigger I, Morizet J, Aubert G, et al. Poly(ethylene glycol)-coated hexadecylcyanoacrylate nanospheres display a combined effect for brain tumor targeting. *J Pharmacol Exp Ther* 2002; 303(3): 928–936.
21. Tsai M-H, Cook JA, Chandramouli GVR, et al. Gene Expression profiling of breast, prostate, and glioma cells following single versus fractionated doses of radiation. *Cancer Res* 2007; 67(8): 3845–3852.
22. Kim JH, Khil MS, Kolozsvary A, et al. Fractionated radiosurgery for 9L gliosarcoma in the rat brain. *Int J Radiat Oncol Biol Phys* 1999; 45(4): 1035–1040.
23. Sharma US, Sharma A, Chau RI, et al. Liposome-mediated therapy of intracranial brain tumors in a rat model. *Pharm Res* 1997; 14(8): 992–998.
24. Heldin C-H, Rubin K, Pietras K, et al. High interstitial fluid pressure – an obstacle in cancer therapy. *Nat Rev Cancer* 2004; 4(10): 806–813.
25. Liu H-L, Hua M-Y, Yang H-W, et al. Magnetic resonance monitoring of focused ultrasound/magnetic nanoparticle targeting delivery of therapeutic agents to the brain. *Proc Natl Acad Sci USA* 2010; 107(34): 15205–15210.
26. Hadjipanayis CG, Fellows-Mayle W and Deluca NA. Therapeutic efficacy of a herpes simplex virus with radiation or temozolomide for intracranial glioblastoma after convection-enhanced delivery. *Mol Ther* 2008; 16(11): 1783–1788.

27. Longmire M, Choyke PL and Kobayashi H. Clearance properties of nano-sized particles and molecules as imaging agents: considerations and caveats. *Nanomedicine (Lond)* 2008; 3(5): 703–717.
28. Choi HS, Liu W, Misra P, et al. Renal clearance of quantum dots. *Nat Biotechnol* 2007; 25(10): 1165–1170.
29. Faure A-C, Dufort S, Josserand V, et al. Control of the in vivo biodistribution of hybrid nanoparticles with different poly(ethylene glycol) coatings. *Small* 2009; 5(22): 2565–2575.